

Gypsum crystals observed in experimental and natural sea ice

N.-X. Geilfus,^{1,2} R. J. Galley,¹ M. Cooper,³ N. Halden,³ A. Hare,¹ F. Wang,^{1,4}
D. H. Sogaard,^{5,6} and S. Rysgaard^{1,2,3,5}

Received 25 October 2013; revised 4 December 2013; accepted 4 December 2013.

[1] Although gypsum has been predicted to precipitate in sea ice, it has never been observed. Here we provide the first report on gypsum precipitation in both experimental and natural sea ice. Crystals were identified by X-ray diffraction analysis. Based on their apparent distinguishing characteristics, the gypsum crystals were identified as being authigenic. The FREZing CHEMistry (FREZCHEM) model results support our observations of both gypsum and ikaite precipitation at typical in situ sea ice temperatures and confirms the “Gitterman pathway” where gypsum is predicted to precipitate. The occurrence of authigenic gypsum in sea ice during its formation represents a new observation of precipitate formation and potential marine deposition in polar seas. **Citation:** Geilfus, N.-X., R. J. Galley, M. Cooper, N. Halden, A. Hare, F. Wang, D. H. Sogaard, and S. Rysgaard (2013), Gypsum crystals observed in experimental and natural sea ice, *Geophys. Res. Lett.*, 40, doi:10.1002/2013GL058479.

1. Introduction

[2] As sea ice forms, dissolved ions become concentrated within sea ice in interstitial liquid brine inclusions leading to significant changes in the mineral-liquid thermodynamic equilibrium and sequential mineral precipitation. Based on experimental work of *Ringer* [1906] and *Nelson and Thompson* [1954], the solid phases that precipitate during seawater freezing are the following hydrated salts: mirabilite ($\text{Na}_2\text{SO}_4 \cdot 10\text{H}_2\text{O}$) at -8.2°C , hydrohalite ($\text{NaCl} \cdot 2\text{H}_2\text{O}$) at -22.9°C , sylvite (KCl), and $\text{MgCl}_2 \cdot 12\text{H}_2\text{O}$ at -36°C and antarcticite ($\text{CaCl}_2 \cdot 6\text{H}_2\text{O}$) at -54°C . This sequence of salt precipitation is known as the “Ringer-Nelson-Thompson pathway.” Experimental and theoretical works supported this pathway for seawater freezing [*Richardson*, 1976; *Herut et al.*, 1990; *Spencer et al.*, 1990; *Marion and Grant*,

1994]. However, the experimental work of *Gitterman* [1937] suggested an alternative pathway where gypsum ($\text{CaSO}_4 \cdot 2\text{H}_2\text{O}$) could precipitate during seawater freezing, likely around -15°C . *Marion et al.* [1999] confirmed this pathway theoretically using a thermodynamic equilibrium model (FREZCHEM) and experimentally using artificial seawater with a composition similar to natural seawater, though in that work gypsum precipitation occurred at -22°C . Adding to this sequential mineral precipitation, *Assur* [1960] suggested that calcium carbonate, as ikaite ($\text{CaCO}_3 \cdot 6\text{H}_2\text{O}$), could precipitate in sea ice at a temperature of -2.2°C .

[3] To our best knowledge, only ikaite precipitation has been formally reported in sea ice. *Light et al.* [2003] reported mirabilite crystals in natural sea ice but without methodological or analytical details. Their core samples were first shipped in dry ice and then stored for 3 years, which may have affected the mineral-liquid thermodynamic equilibrium in the samples. *Alvarez-Aviles et al.* [2008] suggested, based on sulfate enrichment factors, a precipitation of mirabilite in frost flowers (FF) but did not observe any crystals. The question of which polymorph of CaCO_3 would precipitate in natural sea ice was long the subject of debate. But since the recent discovery of ikaite crystals in natural sea ice [*Dieckmann et al.*, 2008], ikaite precipitation has received growing attention due to its role on the carbonate chemistry in sea ice [e.g., *Rysgaard et al.*, 2011; *Geilfus et al.*, 2012, 2013; *Rysgaard et al.*, 2013]. Ikaite has since been included in the FREZCHEM model [*Marion et al.*, 2009].

[4] We provide the first observation of in situ gypsum precipitation in sea ice, associated with ikaite crystals, in both natural and experimental sea ice. We compare our observations with the FREZCHEM model (v13.3) [*Marion et al.*, 2010] and discuss the implication of this precipitation with regard to the “Gitterman pathway” for seawater freezing.

2. Methods

[5] Sampling was performed in both experimental sea ice at the Sea-ice Environmental Research Facility (SERF) site (University of Manitoba) and in fast sea ice in Young Sound near Daneborg, in NE Greenland (74°N , 20°W). The SERF is an outdoor sea ice pool: 18.3 m by 9.1 m in surface area and 2.6 m deep. The pool is exposed to ambient temperatures and to wind and solar radiation by retracting its roof. Artificial seawater used for the experiment was formulated for a final salinity of 27 (Table S1 in the supporting information). While the concentrations of Na^+ and Cl^- of SERF seawater closely matched those in a typical $S=27$ natural seawater (estimated based on $S=35$ “standard” seawater), the artificial SERF seawater was deficient in Mg^{2+} (58% less), SO_4^{2-} (40% less), and Ca^{2+} (17% less) and enriched in TA (45% more). The experimental sea ice and brine exhibited similar physical and chemical properties to those observed in natural

Additional supporting information may be found in the online version of this article.

¹Centre for Earth Observation Science, University of Manitoba, Winnipeg, Manitoba, Canada.

²Arctic Research Centre, Aarhus University, Aarhus, Denmark.

³Department of Geological Sciences, University of Manitoba, Winnipeg, Manitoba, Canada.

⁴Department of Chemistry, University of Manitoba, Winnipeg, Manitoba, Canada.

⁵Greenland Climate Research Centre, Greenland Institute of Natural Resources, Nuuk, Greenland.

⁶Department of biology, University of Southern Denmark, Odense, Denmark.

Corresponding author: N.-X. Geilfus, Arctic Research Centre, Aarhus University, Aarhus, 8000, Denmark. (Geilfus@biology.au.dk)

©2013. The Authors.

This is an open access article under the terms of the Creative Commons Attribution-NonCommercial-NoDerivs License, which permits use and distribution in any medium, provided the original work is properly cited, the use is non-commercial and no modifications or adaptations are made. 0094-8276/13/10.1002/2013GL058479

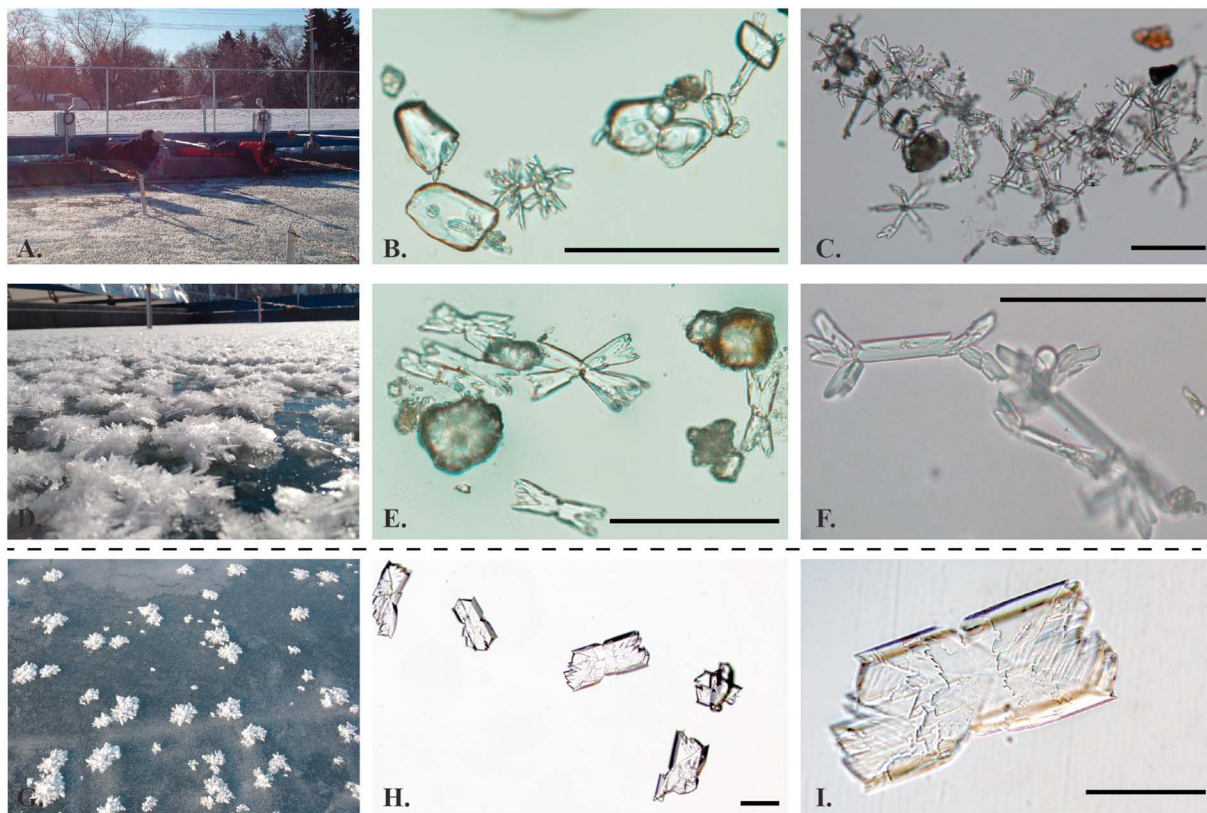


Figure 1. (a) Pictures of the SERF pool covered with FF, (b) mixture of ikaite and gypsum crystals found in SERF ice, (c) mixture of ikaite and gypsum crystals found in SERF FF, (d) closer view of the SERF ice surface covered by FF, (e) gypsum crystals from sea ice samples, (f) gypsum crystals from BS samples. In NE Greenland, (g) sampling site, (h, i) gypsum crystals from sea ice samples. Pictures of ikaite crystals in the NE Greenland site have been fully described by *Rysgaard et al.* [2013]. The bar scale is 50 μm .

Arctic sea ice [*Hare et al.*, 2013]. The NE Greenland site was thin fast ice (15–30 cm thick), less than a week old and covered by FF. This site was chosen as a natural location for new ice growth as it was located in a polynya, where sea ice regularly breaks up due to dynamic forcing.

[6] The SERF experiment took place from 10 to 12 February 2012. We took triplicate samples, once a day, as soon as the initial formation of ice and FF started. Temperatures were measured in situ using a calibrated temperature probe (Testo 720®). FF and brine skim (BS) were collected with a precleaned ceramic-bladed knife, while sea ice samples were collected using a precleaned steel handsaw. Samples were packed in clean plastic bags and kept frozen (below -25°C) until analyzed within a few hours. Seawater underneath the ice was sampled for total alkalinity (TA) and total dissolved inorganic carbon (TCO_2) with a glass syringe fitted with a gastight Tygon tube inserted through a core hole. Samples were poisoned with a solution of saturated HgCl_2 and stored in the dark at 4°C until analysis. Subsamples of sea ice, BS, and FF were melted in the laboratory at 20°C for salinity measurements using a Thermo Orion 3-star with an Orion 013610MD conductivity cell and values were converted to bulk salinity [*Grasshoff et al.*, 1983].

[7] In NE Greenland, FF and BS were collected with a precleaned ceramic-bladed knife and stored in clean plastic bags at -20°C until further processing within few hours. Triplicate sea ice samples were collected using a MARK II coring system (Kovacs Enterprises). Vertical temperature

profiles were measured directly after extraction of the first core using a calibrated temperature probe (Testo 720®) inserted into holes (~ 3 cm deep) drilled perpendicular to the vertical axis of the ice core. The sea ice was cut in 5 cm sections and kept cold in transit to the field laboratory within 1 h for further analysis. These sea ice sections were melted in the 20°C laboratory for salinity measurements as described previously.

[8] Ikaite crystals were observed and sampled using two techniques. At SERF, we used the method developed by *Dieckmann et al.* [2008]; subsamples of sea ice, FF, and BS were melted in a fridge at 2°C . Crystals were pipetted, transferred in a gastight vial (12 ml Exetainer®, Labco High Wycombe, UK) filled with 75% ethanol, and stored at -20°C for further analysis. In Greenland we used a technique developed by *Rysgaard et al.* [2013] where ice samples were placed onto a glass slide, brought into the field laboratory within few hours of ice coring, and inspected under a microscope (Leica DMiL LED) as the samples melted. Sea ice cores were brought back to the University of Manitoba for further identification of the crystals at the X-ray laboratory in the Department of Geological Sciences. Both gypsum and ikaite crystal morphology as determined under microscopic examination remained the same in the field as during later examination in the X-ray laboratory at the University of Manitoba, Canada.

[9] In the X-ray laboratory, a small droplet of ethanol-containing crystals from SERF and Greenlandic subsamples was deposited onto a cold glass slide resting on a chilled

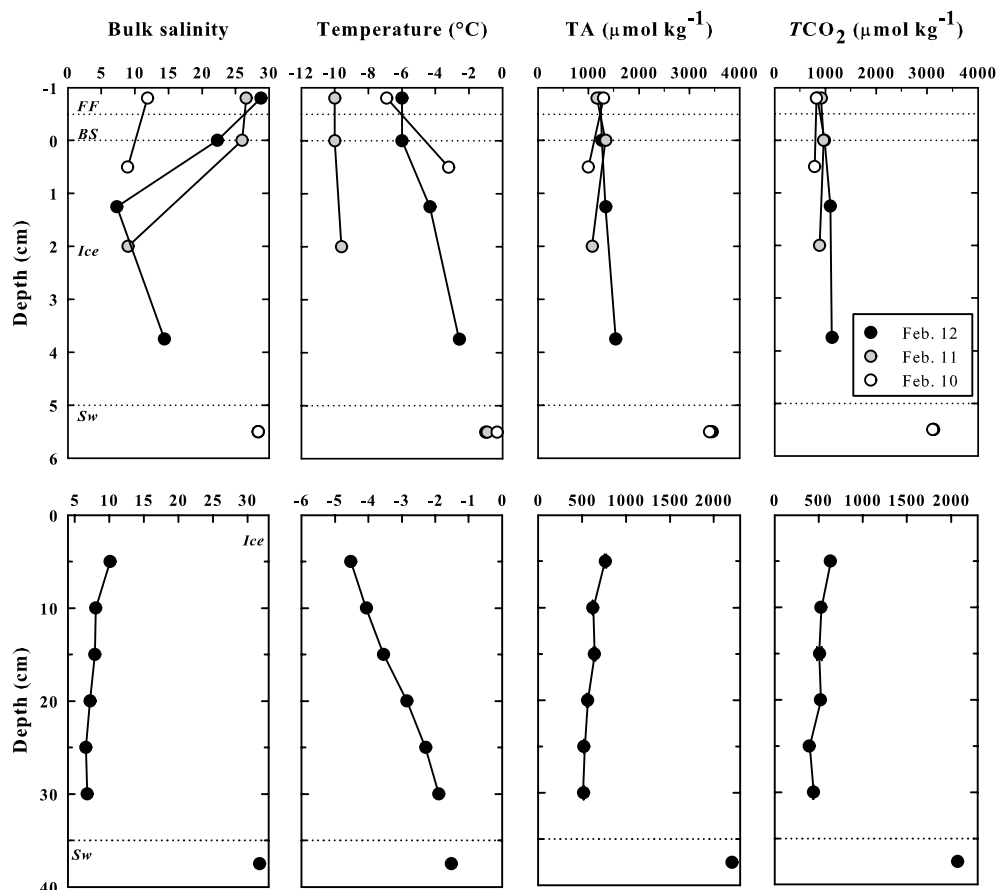


Figure 2. Profiles of bulk salinity, temperature ($^{\circ}\text{C}$), total alkalinity, and total dissolved inorganic carbon (in $\mu\text{mol kg}^{-1}$) from (top row) SERF experiment and (bottom row) NE Greenland. TA and TCO_2 concentrations from Greenland are an average of three samples with a standard deviation of less than 5%.

aluminum block containing a 1 cm central-viewing hole. The crystals were examined with a microscope under polarized light to assess their optical properties and then mounted for X-ray study using a stereo binocular microscope. Crystals were dragged across the cold glass slide from the water droplet and immersed into a drop of special purpose oil to restrict sublimation. Each crystal was then rapidly transferred with a low X-ray scattering microloop to the nitrogen cold stream (-20°C) of the X-ray diffraction instrument with a magnetic coupling goniometer head. The X-ray diffraction instrument consisted of a Bruker D8 three-circle diffractometer equipped with a rotating anode generator (*MoK α* X-radiation), multi-layer optics, APEX-II CCD detector, and an Oxford 700 Series liquid-N Cryostream. The intensities of more than 100 reflections were harvested from six frame series (each spanning 15° in either ω or ϕ) collected to 60° 2θ using 0.6 s per 1° frame with a crystal-to-detector distance of 5 cm. In total, a dozen crystals (from sea ice, FF, and BS) from both sampling sites were identified through successful indexing of observed x-ray diffraction maxima onto known characteristic unit cells.

[10] TCO_2 and TA concentrations in sea ice, FF, and BS samples were measured from SERF and NE Greenland by placing samples in gastight laminated (Nylon, ethylene vinyl alcohol, and polyethylene) plastic bags [Hansen *et al.*, 2000] fitted with a gastight Tygon tube and a valve for sampling. 50 μl of a saturated solution of HgCl_2 was then added to the samples. Samples were melted in the dark at 2°C over 48 h

to 72 h. The meltwater was then transferred to a gastight vial (12 ml Exetainer $^{\circledR}$). TCO_2 concentrations were measured on a coulometer [Johnson *et al.*, 1987], and TA was measured by potentiometric titration [Haraldsson *et al.*, 1997]. Routine analysis of Certified Reference Materials provided by A. G. Dickson, Scripps Institution of Oceanography, verified that TCO_2 and TA could be analyzed within ± 2 and 3 $\mu\text{mol kg}^{-1}$, respectively.

[11] Formation of gypsum and ikaite was modeled by FREZCHEM (version 13.3), an equilibrium chemical thermodynamic model parameterized for concentrated solutions (up to 20 mol kg^{-1} H_2O) and subzero temperatures (down to -70°C) [Marion *et al.*, 2010]. The model uses the Pitzer approach to correct for activity coefficients of solutes in concentrated solutions. All the thermodynamic constants used were the default values provided by the model [Marion, 2001]. While the FREZCHEM mineral database includes a variety of stable and metastable carbonate minerals of Ca (e.g., calcite, dolomite, aragonite, and vaterite), only ikaite was considered in these calculations because the equilibrium model would otherwise always select the most stable carbonate minerals. The model inputs included the concentrations of all the major ions and the values of salinity and TA. Two types of seawater were considered: (i) “standard seawater” ($S=35$, $\text{TA}=2390 \mu\text{mol kg}^{-1}$) and (ii) less saline seawater similar in composition as the seawater in Young Sound, NE Greenland ($S=31$, $\text{TA}=2116 \mu\text{mol kg}^{-1}$). The model froze seawater from 0 to -25°C by 0.1°C increments. We assume

that during the freezing process the system is always open to a constant $p\text{CO}_2 = 390 \mu\text{atm}$ and that solid phases precipitated at any given temperature are allowed to dissolve and reprecipitate as different solids with temperature changes (“equilibrium crystallization”). It should be noted that the FREZCHEM model simulates the formation of ice, along with other possible minerals, as seawater freezes in a system “closed” with respect to matter except for gaseous component (in this case CO_2), which is allowed to transfer into or out of the system.

3. Results

[12] During the experiment, large and well-formed FF grew and covered the sea ice surface (Figure 1a). The sea ice thickness was a few millimeters on February 10 and increased to a maximum ice thickness of 5 cm on February 12. Sea ice temperature ranged from -10°C immediately above the sea ice interface with the atmosphere to -3.3°C nearest of the sea ice interface with the underlying seawater. The salinity of the ice stayed relatively constant around 9 while the salinity of the FF increased from 12 to 29 (Figure 2) over the 3 day period. TA and TCO_2 from seawater increased slightly from 3397 to $3457 \mu\text{mol kg}^{-1}$ and 3108 to $3124 \mu\text{mol kg}^{-1}$, respectively. This increase also occurred within sea ice where TA and TCO_2 increased from 999 to $1539 \mu\text{mol kg}^{-1}$ and 791 to $1128 \mu\text{mol kg}^{-1}$, respectively. Within the BS and FF, TA and TCO_2 ranged from 1169 to $1340 \mu\text{mol kg}^{-1}$ and 791 to $1128 \mu\text{mol kg}^{-1}$, respectively.

[13] In NE Greenland, the ice temperature was -5°C near the air-ice interface with a gradient to -1.9°C near the sea ice-seawater interface (Figure 2). Bulk ice salinity ranged from 10 at 5 cm depth to 6.8 at 30 cm depth. TA and TCO_2 concentrations in sea ice ranged from 766 to $517 \mu\text{mol kg}^{-1}$ and 630 to $440 \mu\text{mol kg}^{-1}$, respectively. TA and TCO_2 of the underlying seawater were 2206 and $2073 \mu\text{mol kg}^{-1}$.

[14] At both sites, two kinds of crystals (10 to $150 \mu\text{m}$) with different shapes were observed in newly formed sea ice, BS, and FF. We found highly transparent crystals with a rhombic morphology (Figures 1b and 1c), which showed uniform extinction under cross-polarized light, suggesting that they were simple single crystals. All reflections fitted well to a monoclinic C-centered cell with (a)= 8.814 , (b)= 8.315 , (c)= 11.037 , β = 110.615 , and V = 757.13 . From their general appearance and unit cell determination, these crystals were confirmed to be ikaite [Hesse and Koppers, 1983]. We also observed crystals with very different morphology and optical properties. These crystals were highly transparent, thin, and elongated (up to $100 \mu\text{m}$, Figures 1d–1f, 1h, and 1i). The X-ray analysis showed that all reflections fitted well to a monoclinic C-centered cell with (a)= 6.280 , (b)= 15.189 , (c)= 5.678 , β = 114.208 , and V = 494.0 . From the unit cell determination these crystals were identified as gypsum ($\text{CaSO}_4 \cdot 2\text{H}_2\text{O}$) [Pedersen and Semmingsen, 1982]. The gypsum crystals were euhedral, and most of them were intergrown (twinned) either at right angles or as intergrown rosettes, with a fishtail-like appearance on each extremity in both cases. The texture of the gypsum crystals was planar. Some crystals presented breakage surfaces.

[15] Both the ikaite and gypsum crystals had distinct morphology and were easily recognized. Ikaite and gypsum crystals were distributed throughout the entire sea ice and in FF and BS, with higher proportions of larger crystals

(> $100 \mu\text{m}$ size) in the FF. After a few minutes at room temperature, ikaite crystals disaggregated into a multitude of smaller crystal components. In contrast, gypsum crystals remained stable and did not dissolve at room temperature.

4. Discussion

[16] Precipitation of ikaite and gypsum was observed at both locations and within hours of initial sea ice formation. For the first time, gypsum crystals ($\text{CaSO}_4 \cdot 2\text{H}_2\text{O}$) have been observed in experimental sea ice and in natural sea ice, easily distinguished from ikaite crystals based on their morphological differences. Both types of crystals were found through the entire sea ice column, in FF and in BS. Usually, detrital gypsum is distinguished from authigenic gypsum on the basis of grain morphology with detrital gypsum occurring as subhedral crystals with cleaved and abraded surfaces and authigenic gypsum occurring as euhedral unbroken crystals [Rothwell, 1989]. Based on these distinguishing characteristics, the gypsum identified in this study is authigenic.

[17] Gypsum is a very soft mineral mainly found in sedimentary and evaporative environments [Chang et al., 1998]. The generally accepted mechanisms for gypsum formation are the evaporation of seawater, the oxidation of sulfides to sulfate, the action of sulfate-rich acid on carbonate-bearing rocks, and the hydration of anhydrite [Chang et al., 1998]. Gypsum resulting from evaporated seawater is the most common form due to the high-calcium and high-sulfate concentrations (increased by evaporation) of normal seawater [Hoareau et al., 2011]. According to Perovich and Richter-Menge [1994] and Alvarez-Aviles et al. [2008], FF on newly formed sea ice are a mixture of atmospheric moisture and liquid from the BS expelled upward from sea ice during the sea ice growth. The evaporation of highly concentrated brine may be one of the required conditions for ikaite and gypsum precipitation. Mineral precipitation may be enhanced in FF because (i) FF wick up concentrated liquid brine skim by capillary action, (ii) FF have very high surface area from which to evaporate brine rapidly, and (iii) FF are cold enough to precipitate ikaite and gypsum. Also, high concentrations of calcium and sulfate promote both the precipitation of ikaite [Bischoff et al., 1993; Buchardt et al., 2001] and gypsum [Hoareau et al., 2011].

[18] Gitterman [1937] suggested that gypsum could precipitate at -15°C during seawater freezing. Marion et al. [1999] confirmed this precipitation but at a temperature of -23°C . In this study we observed gypsum precipitation in a temperature window from -3.2°C to -10°C . The FREZCHEM model (version 13.3) shows the precipitation of gypsum and ikaite crystals using both average seawater composition [Millero, 2006] and seawater similar in composition as in Young Sound, NE Greenland. For standard seawater, the model predicts ikaite precipitation at -4.9°C and mirabilite precipitation at -6.4°C . Gypsum is predicted to precipitate at $T \leq -21.9^\circ\text{C}$, which is consistent with previous work [i.e., Marion and Farren, 1999; Marion et al., 1999, 2010]. However, small amounts of gypsum are also predicted to form within a second, narrow temperature window between -6.2 and -7.1°C , making gypsum the first sulfate mineral to precipitate as seawater freezes. The subsequent precipitation of mirabilite (at -6.4°C) decreases sulfate molality causing gypsum to be dissolved when the temperature is slightly lower (-7.1°C). Once the temperature is substantially low ($\leq -21.9^\circ\text{C}$), the dissolution of mirabilite increases the sulfate molality causing gypsum to precipitate again [Marion

and Farren, 1999]. Similar results were obtained when modeling the freezing of the NE Greenland seawater. The second lower temperature window for gypsum precipitation is in the same range as observed here in both SERF and in NE Greenland, supporting our observations of gypsum precipitation at typical in situ sea ice temperatures. The high sensitivity of gypsum in the warmer (-6.2 and -7.1°C) temperature window due to competition with mirabilite for sulfate probably explains why gypsum has not been commonly reported by previous studies. It may also be that previous studies (e.g., Dieckmann *et al.*, [2008] and Geilfus *et al.*, [2013] among others) were focused on ikaite without the foresight to look into detail for gypsum among other precipitates. As a result of the small width of its warmer temperature window, it could easily be missed due to sampling at suboptimal temperatures for its precipitation. Further, even if it was present, its abundance might have been so low as to be neglected, especially without actively searching for it. The amount of time allowed for samples to melt may affect the presence of gypsum, as temperature and contact with atmospheric CO_2 greatly affect the stability of these gypsum precipitates among other crystals. Finally, the brine saturation with respect to the various minerals over a range of temperatures may prove important and is the topic of work in preparation, requiring further development of the FREZCHEM model.

[19] Compared to natural seawater, freezing SERF seawater is a less likely medium for gypsum precipitation: lower concentrations of SO_4^{2-} and Ca^{2+} are unfavorable to gypsum precipitation and high TA enhances ikaite production, which further lowers the concentration of Ca^{2+} . So observation of gypsum precipitation under unfavorable conditions suggests that gypsum precipitation in sea ice could be a robust and widespread phenomenon under certain temperature ranges.

[20] Gypsum is not usually found as a constituent of deep marine sediments, reflecting the typical condition that seawater is undersaturated with respect to gypsum [Briskin and Schreiber, 1978], but it has been found as a minor constituent in sediment from two deepwater Ocean Drilling Program sites, one in the SE Greenland and one in the Gulf of Alaska [John and Cowan, 2000]. The occurrence of gypsum in these marine cores is unusual and unexpected considering their cold climate and the high latitude [John and Cowan, 2000]. Investigations into whether these gypsum crystals are authigenic or detrital could provide a new model for precipitate formation and marine deposition in polar seas influenced by sea ice formation. Finally, more work on the link between gypsum precipitation in sea ice and the subsequent vertical export to the sea floor is needed as it may provide a proxy record on previous sea ice conditions.

5. Conclusions

[21] We observed similar processes occurring in an artificial sea ice tank (the Sea-ice Environment Research Facility (SERF) at the University of Manitoba, Winnipeg, Canada) and in young (< 30 cm) fast sea ice in NE Greenland. At both sites, precipitation of ikaite crystals was observed as soon as the ice started to grow, and gypsum crystals were observed for the first time within sea ice, BS, and FF.

[22] The FREZCHEM model results support our observations of ikaite and gypsum precipitation (provided mirabilite is not formed in high amounts) at typical in situ sea ice temperatures. The occurrence of authigenic gypsum in sea ice during its formation represents a new observation of precipitate

formation and potential marine deposition in polar seas. Gypsum precipitating during sea ice growth may eventually sink and accumulate in the sea floor, which might provide a proxy record for past ice conditions.

[23] **Acknowledgments.** The Canada Excellence Research Chair (CERC) funded this study. SERF was funded by the Canada Foundation of Innovation (CFI), the Manitoba Research and Innovation Fund, and the University of Manitoba. DHS was financially supported by the commission for scientific Research in Greenland (KVUG). We would like to thank Giles Marion for his assistance with version 13.3 of FREZCHEM and for his review of the manuscript, as well as an anonymous reviewer. N.-X.G. would like to thank D. Thomas for his advice. This work is a contribution to the Arctic Science Partnership (ASP), asp-net.org.

[24] The Editor thanks two anonymous reviewers for their assistance in evaluating this paper.

References

- Alvarez-Aviles, L., W. R. Simpson, T. A. Douglas, M. Sturm, D. Perovich, and F. Domine (2008), Frost flower chemical composition during growth and its implications for aerosol production and bromine activation, *J. Geophys. Res.*, *113*, D21304, doi:10.1029/2008JD010277.
- Assur, A. (1960), Composition of sea ice and its tensile strength, *SIPRE Research Report 44*.
- Bischoff, J. L., J. A. Fitzpatrick, and R. J. Rosenbauer (1993), The solubility and stabilization of ikaite ($\text{CaCO}_3 \cdot 6\text{H}_2\text{O}$) from 0°C to 25°C environmental and paleoclimatic implications for Thimolite Tufa, *J. Geol.*, *101*(1), 21–33.
- Briskin, M., and B. C. Schreiber (1978), Authigenic gypsum in marine sediments, *Mar. Geol.*, *28*, 37–49.
- Buchardt, B., C. Israelson, P. Seaman, and G. Stockmann (2001), Ikaite tufa towers in Ikka Fjord, southwest Greenland: Their formation by mixing of seawater and alkaline spring water, *J. Sediment. Res.*, *71*(1), 176–189.
- Chang, L. L. Y., R. A. Howie, and J. Zuusman (1998), *Rock-Forming Minerals*, vol. 5B, Non-Silicates, 383 pp., The Geological Society, London.
- Dieckmann, G. S., G. Nehrke, S. Papadimitriou, J. Gottlicher, R. Steininger, H. Kennedy, D. Wolf-Gladrow, and D. N. Thomas (2008), Calcium carbonate as ikaite crystals in Antarctic sea ice, *Geophys. Res. Lett.*, *35*, L08501, doi:10.1029/2008GL033540.
- Geilfus, N. X., G. Carnat, T. Papakyriakou, J. L. Tison, B. Else, H. Thomas, E. Shadwick, and B. Delille (2012), Dynamics of pCO_2 and related air-ice CO_2 fluxes in the Arctic coastal zone (Amundsen Gulf, Beaufort Sea), *J. Geophys. Res.*, *117*, C00G10, doi:10.1029/2011JC007118.
- Geilfus, N. X., G. Carnat, G. S. Dieckmann, N. Halden, G. Nehrke, T. Papakyriakou, J. L. Tison, and B. Delille (2013), First estimates of the contribution of CaCO_3 precipitation to the release of CO_2 to the atmosphere during young sea ice growth, *J. Geophys. Res. Oceans*, *118*, 244–255, doi:10.1029/2012JC007980.
- Gitterman, K. E. (1937), *Thermal Analysis of Sea Water*, USA Cold Regions Research and Engineering Laboratory, Hanover, NH.
- Grasshoff, K., M. Ehrhardt, and K. Kremling (1983), *Methods of Sea Water Analysis*, Verlag Chemie, Weinheim, Germany.
- Hansen, J. W., B. Thamdrup, and B. B. Jørgensen (2000), Anoxic incubation of sediment in gas-tight plastic bags: A method for biogeochemical processes studies, *Mar. Ecol. Prog. Ser.*, *208*, 273–282.
- Haraldsson, C., L. G. Anderson, M. Hasselov, S. Hulth, and K. Olsson (1997), Rapid, high-precision potentiometric titration of alkalinity in ocean and sediment pore waters, *Deep Sea Res., Part 1*, *44*(12), 2031–2044.
- Hare, A. A., F. Wang, D. Barber, N. X. Geilfus, R. J. Galley, and S. Rysgaard (2013), pH evolution in sea ice grown at an outdoor experimental facility, *Mar. Chem.*, *154*, 46–54.
- Herut, B., A. Starinsky, A. Katz, and A. Bein (1990), The role of seawater freezing in the formation of subsurface brines, *Geochim. Cosmochim. Acta*, *54*(1), 13–21.
- Hesse, K.-F., and H. Kuppers (1983), Refinement of the structure of Ikaite, $\text{CaCO}_3 \cdot 6\text{H}_2\text{O}$, *Z. Kristallogr.*, *163*, 227–231.
- Hoareau, G., C. Monnin, and F. Odonne (2011), The stability of gypsum in marine sediments using the entire ODP/IODP porewater composition database, *Mar. Geol.*, *279*, 87–97.
- John, K. E. K. S., and E. A. Cowan (2000), Terrestrial gypsum from Alaska and Greenland in glacially influenced marine sediments, *Sediment. Geol.*, *136*, 43–58.
- Johnson, K. M., J. M. Sieburth, P. J. L. Williams, and L. Brandstrom (1987), Coulometric total carbon dioxide analysis for marine studies: Automation and calibration, *Mar. Chem.*, *21*(2), 117–133.

- Light, B., G. A. Maykut, and T. C. Grenfell (2003), Effects of temperature on the microstructure of first-year Arctic sea ice, *J. Geophys. Res.*, *108*(C2), 3051, doi:10.1029/2001JC000887.
- Marion, G. M. (2001), Carbonate mineral solubility at low temperatures in the Na-K-Mg-Ca-H-Cl-SO₄-OH-HCO₃-CO₃-CO₂-H₂O system, *Geochim. Cosmochim. Acta*, *65*(12), 1883–1896.
- Marion, G. M., and R. E. Farren (1999), Mineral solubilities in the Na-K-Mg-Ca-Cl-SO₄-H₂O system: A re-evaluation of the sulfate chemistry in the Spencer-Moller-Weare model, *Geochim. Cosmochim. Acta*, *63*(9), 1305–1318.
- Marion, G. M., and S. A. Grant (1994), FREZCHEM: A chemical-thermodynamic model for aqueous solutions at subzero temperatures, *CRREL Spec. Rep.*
- Marion, G. M., R. E. Farren, and A. J. Komrowski (1999), Alternative pathways for seawater freezing, *Cold Reg. Sci. Technol.*, *29*(3), 259–266.
- Marion, G. M., F. J. Millero, and R. Feistel (2009), Precipitation of solid phase calcium carbonates and their effect on application of seawater S-A-T-P models, *Ocean Sci.*, *5*(3), 285–291.
- Marion, G. M., M. V. Mironenko, and M. W. Roberts (2010), FREZCHEM: A geochemical model for cold aqueous solutions, *Comput. Geosci.*, *36*(1), 10–15.
- Millero, F. J. (2006), *Chemical Oceanography*, 3rd ed., CRC Press, Taylor and Francis Group, Boca Raton, FL.
- Nelson, K. H., and T. G. Thompson (1954), Deposition of salts from sea water by frigid concentration, *J. Mar. Res.*, *13*, 166–182.
- Pedersen, B. F., and D. Semmingsen (1982), Neutron-diffraction refinement of the structure of gypsum, CaSO₄·2H₂O, *Acta Crystallogr., Sect. B Struct. Sci.*, *38*(Apr), 1074–1077.
- Perovich, D. K., and J. A. Richter-Menge (1994), Surface characteristics of lead ice, *J. Geophys. Res.*, *99*(C8), 16,341–16,350.
- Richardson, C. (1976), Phase relationships in sea ice as a function of temperature, *J. Glaciol.*, *17*(77), 507–519.
- Ringer, W. E. (1906), De veranderingen in samenstelling van zeewater bij het bevriezen [changes in the composition of sea water upon freezing], *Chem. Weekblad*, *3*, 223–249.
- Rothwell, R. G. (Ed) (1989), *Minerals and Mineraloids in Marine Sediments*, 279 pp., Elsevier, London.
- Rysgaard, S., J. Bendtsen, B. Delille, G. S. Dieckmann, R. N. Glud, H. Kennedy, J. Mortensen, S. Papadimitriou, D. N. Thomas, and J. L. Tison (2011), Sea ice contribution to the air-sea CO₂ exchange in the Arctic and Southern Oceans, *Tellus, Ser. B*, *63*(5), 823–830.
- Rysgaard, S., et al. (2013), Ikaite crystal distribution in winter sea ice and implications for CO₂ system dynamics, *The Cryosphere*, *7*, 707–718.
- Spencer, R. J., N. Møller, and J. H. Weare (1990), The prediction of mineral solubilities in natural waters: A chemical equilibrium model for the Na-K-Ca-Mg-Cl-SO₄-H₂O system at temperature below 25°C, *Geochim. Cosmochim. Acta*, *54*(3), 575–590.